ELSEVIER

Biochimica et Biophysica Acta 1415 (1998) 135–146

BIOCHIMICA ET BIOPHYSICA ACTA

BBA

Interaction of the neuronal marker dye FM1-43 with lipid membranes Thermodynamics and lipid ordering

Uwe Schote, Joachim Seelig *

Department of Biophysical Chemistry, Biocenter of the University of Basel, Klingelbergstr. 70, CH-4056 Basel, Switzerland

Received 16 July 1998; accepted 2 October 1998

Abstract

The fluorescent dye FM1-43 labels nerve terminals in an activity-dependent fashion and has been found increasingly useful in exploring the exo- and endocytosis of synaptic vesicles and other cells by fluorescence methods. The dye distributes between the aqueous phase and the lipid membrane but the physical-chemical parameters characterizing the adsorption/partition equilibrium have not yet been determined. Fluorescence spectroscopy alone is not sufficient for a detailed elucidation of the adsorption mechanism since the method can be applied only in a rather narrow low-concentration window. In addition to fluorescence spectroscopy, we have therefore employed high sensitivity isothermal titration calorimetry (ITC) and deuterium magnetic resonance (^{2}H-NMR). ITC allows the measurement of the adsorption isotherm up to 100 μM dye concentration whereas ^{2}H-NMR provides information on the location of the dye with respect to the plane of the membrane. Dye adsorption/partition isotherms were measured for neutral and negatively-charged phospholipid vesicles. A non-linear dependence between the extent of adsorption and the free dye concentration was observed. Though the adsorption was mainly driven by the insertion of the non-polar part of the dye into the hydrophobic membrane interior, the adsorption equilibrium was further modulated by an electrostatic attraction/repulsion interaction of the cationic dye ($z=+2$) with the membrane surface. The Gouy-Chapman theory was employed to separate electrostatic and hydrophobic effects. After correcting for electrostatic effects, the dye-membrane interaction could be described by a simple partition equilibrium ($X_b = Kc_{dye}$) with a partition constant of 10^3–10^4 M^{-1}, a partition enthalpy of $\Delta H = -2.0$ kcal/mol and a free energy of binding of $\Delta G = -7.8$ kcal/mol. The insertion of FM1-43 into lipid membranes at room temperature is thus an entropy-driven reaction following the classical hydrophobic effect. Deuterium nuclear magnetic resonance provided insight into the structural changes of the lipid bilayer induced by the insertion of FM1-43. The dye disturbed the packing of the fatty acyl chains and decreased the fatty acyl chain order. FM1-43 also induced a conformational change in the phosphocholine headgroup. The $^-$P-N$^+$ dipole was parallel to the membrane surface in the absence of dye and was rotated with its positive end towards the water phase upon dye insertion. The extent of rotation was, however, much smaller than that induced by other cationic molecules of similar charge, suggesting an alignment of FM1-43 such that the POPC phosphate group is sandwiched by the two quaternary FM1-43 ammonium groups. In such an arrangement the two cationic charges counteract each other in a rotation of the $^-$P-N$^+$ dipole.

Keywords: Lipid ordering; Thermodynamics; Neuronal marker dye; FM1-43

1. Introduction

The optical monitoring of neuronal activity in vivo and in vitro with fluorescence dyes has become a

* Corresponding author. Fax: +41 (61) 267-2189; E-mail: seelig1@ubaclu.unibas.ch

0005-2736/98/$ – see front matter
PII: S0005-2736(98)00188-6

powerful method in neurobiology. A change in the membrane potential of nerve cells stained with a voltage-sensitive dye is accompanied by changes in optical properties, usually absorption or fluorescence [1–3]. The most sensitive dyes are those of the merocyanine, oxonol, and cyanine families (especially styryl dyes) [4]. A good optical probe is characterized by a high voltage sensitivity, but also by the absence of photodynamic damage and pharmacological side effects [5]. Different mechanisms, e.g. dye movement, dye aggregation, changes in the properties of the membrane, and most important electrochromism, have been postulated to couple a rapid change in the membrane potential to a spectral response [2,4].

A recent application of styryl dyes is the non-toxic, activity-dependent fluorescent labeling of living nerve terminals. The dye FM1-43 was found to be particularly useful since an effective staining of the synaptic vesicles within nerve terminals was achieved if the nerve was electrically stimulated [6]. FM1-43 has become a tool for optically monitoring the complete cycle of synaptic vesicles, i.e. their exocytosis and endocytosis, and for labeling living terminals according to their level of activity [7–12]. Dye molecules become trapped within recycled synaptic vesicles and the measured fluorescence intensity was found to be proportional to the amount of transmitter released [7,8]. Previously stained terminals destain during exocytosis of loaded vesicles [7,8,10]. In addition, it was possible to show that endocytosis was not dependent on the membrane potential and, unlike exocytosis, was also independent of the extracellular Ca^{2+} concentration [10,11]. The mechanism by which FM1-43 stains synaptic vesicles can be described by a combination of two forces: the high affinity of the dye for lipid membranes and its inability to penetrate the membrane because of its electric charge ($z = +2$). The hydrophobic tail of FM1-43 readily dissolves in the lipid membrane but the molecule is prevented from passing through the membrane by two quaternary amino groups. Hence, the dye partitions only into the outer leaflet of membranes, without diffusing through the membrane and entering the cytoplasm [13].

The spectral properties of the dye change according to its environment and are reflected in a dramatic increase of the fluorescence intensity and in a blue shift of the maximum emission wavelength [9] upon incorporation into a cell membrane. Most of the fluorescence signal originates from the interaction with the lipid bilayers and not from that with membrane proteins [3,4,14]. It was further suggested that different neuronal membranes have different bilayer structures and that the dye-membrane interaction can monitor changes in the lipid environment [15].

The purpose of the present study was to analyze the physical-chemical aspects of FM1-43 partitioning into lipid model membranes. Fluorescence and high-sensitivity titration calorimetry were used to obtain insight into the thermodynamics of the dye-membrane binding equilibrium. The calorimetric studies were performed at pH 5.5 and 7.4 and with varying lipid composition, i.e. neutral 1-palmitoyl-2-oleoyl-*sn*-glycero-3-phosphocholine (POPC) and mixtures of POPC with negatively charged 1-palmitoyl-2-oleoyl-*sn*-glycero-3-phosphoglycerol (POPG). Fluorescence spectroscopy and titration calorimetry allowed a measurement of the binding isotherms over a relatively large concentration range. The binding isotherms were then analyzed by applying the Gouy-Chapman theory which allows a separation of hydrophobic and electrostatic contributions to the overall binding [16,17]. The location of the dye molecule with respect to the plane of the lipid membrane was studied with deuterium nuclear magnetic resonance. Deuterium labels were placed at the headgroup segments of phosphatidylcholine lipids and at different positions of the hydrocarbon chains. The segmental fluctuations and the conformational changes were derived from the measured quadrupole splittings.

2. Materials and methods

2.1. Materials

FM1-43 (*N*-(3-triethylammoniumpropyl)-4-(*p*-dibutylaminostyryl)pyridinium-dibromide) was purchased from Molecular Probes (Eugene, OR, USA). The fluorophore concentration was determined by UV spectroscopy using an extinction coefficient $\varepsilon = 52\,000\ M^{-1}\ cm^{-1}$ in methanol at $\lambda = 502$ nm (product information from Molecular Probes).

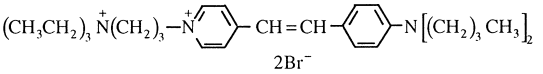

FM1-43

The phospholipids 1-palmitoyl-2-oleoyl-*sn*-glycero-3-phosphocholine (POPC) and 1-palmitoyl-2-oleoyl-*sn*-glycero-3-phosphoglycerol (POPG) were kindly provided by Sandoz (Basel, Switzerland).

For the deuterium NMR measurements POPC was selectively deuterated at the α- and β-segments of the choline headgroup as described previously [18] and (9′,10′-$^2H_2$)POPC was prepared according to Seelig and Waespe-Sarcevic [19]. For the NMR experiments deuterium-depleted water was used.

2.2. NMR measurements

Mixtures of FM1-43 and deuterated POPC were prepared in 8-mm (outer diameter) test tubes. 1–1.5 ml of a POPC stock solution (approx. 20 mg/ml in dichloromethane) was pipetted into the sample tube, and the solvent was evaporated under nitrogen. The dry lipids (under high vacuum over P_2O_5 for several hours) were weighed, and the appropriate volume of an FM1-43 stock solution in methanol was added to achieve the desired molar ratio. After mixing, the solvent was removed and the dried sample was weighed again. The molar ratio of FM1-43 to POPC was calculated from the weights of the dried lipids. The lipid mixtures used for ^{2}H-NMR measurements were dispersed in about 70 μl deuterium-depleted water in order to minimize the isotropic ^{2}H-NMR signal due to the natural abundance of deuterium in water. The dispersions were vortexed and freeze-thawed several times until a homogeneous preparation was achieved. The NMR measurements were carried out at 23°C.

The solid-state NMR measurements of membranes were performed with a Bruker MSL 400 spectrometer operating at 61.4 MHz for ^{2}H. A quadrupole echo sequence with a pulse spacing of 40 μs was used [20]. The π/2 pulse width was 4.2 μs, the sweep width 50 kHz and the recycling delay 250 ms. A total of 5000 FIDs were accumulated.

2.3. Preparation of small unilamellar vesicles

Experiments using fluorescence and UV-spectroscopy or high sensitivity titration calorimetry were performed with unilamellar vesicles composed of either POPC or POPC/POPG mixtures. POPC and POPG were dissolved in dichloromethane and were mixed in the desired ratio. The solvent was evaporated under a stream of nitrogen and the samples were dried overnight in vacuo. Buffer (100 mM NaCl, 10 mM Tris (pH 7.4) or 10 mM phosphate (pH 7.4 or 5.5)) was added to the dry lipid films and the suspensions were vortexed extensively. The lipid dispersions were sonified under nitrogen for about 45 min (at 10°C) to form small unilamellar vesicles (diameter $\approx$30 nm). Metal debris from the titanium tip was removed by centrifugation for 10 min in an Eppendorf centrifuge.

2.4. Calorimetric measurement of reaction enthalpies and binding constants

The thermodynamic binding effects were measured with a Microcal MC-2 high-sensitivity titration calorimeter (Microcal, Northhampton, MA, USA) described in [21]. The solutions were degassed under vacuum prior to use. The calorimeter was calibrated electrically. The data were processed, using the Origin® software developed by Microcal.

The reaction enthalpies were measured by dye-into-lipid titrations. 10-μl aliquots of a dye solution ($c_F \approx 1$ mM) were titrated into the calorimeter cell (1.278 cm^3) filled with lipid suspension ($c_L \approx 12$ mM). The injection syringe was coupled to a digital stepping motor and was rotated at a speed of 400 rot./min. Due to the large excess of lipid and the high affinity of FM1-43 for lipids, all dye was immediately bound to the vesicles. Each injection step provided the complete heat of reaction as determined from the integral over the respective calorimetric trace.

The partition constants were measured by lipid-into-dye titration. The vesicle suspension ($c_L \sim 40$ mM) was injected in 10-μl aliquots into the sample cell filled with dye solution ($c_F \sim 100$ μM). The corresponding heats of reaction decreased with each injection as less and less dye was available for binding. From the variation of the heat of reaction the binding isotherm was derived (cf. Seelig, 1997).

Control experiments were carried out by injecting the dye solution or the lipid vesicles into buffer. All heat signals are corrected for this heat of dilution.

2.5. Fluorescence and UV spectroscopy

Fluorescence measurements were made with a Jas-

co FP-777 spectrofluorometer (excitation at 496 nm, emission in the range 570–650 nm). We measured the emission wavelength λ_{max} and the fluorescence intensities of FM1-43 in the absence of lipid and bound to lipid vesicles. The binding of the dye to phospholipid membranes was accompanied by a strong increase in the fluorescence. The binding constant of the dye-lipid interaction was calculated with a lipid-into-dye experiment by injecting small aliquots of a vesicle suspension ($c_L = \sim 2$ mM) into a cuvette with dye solution ($c_F = \sim 0.5$–2 μM). The cuvette was shaken several times and the fluorescence intensity was measured after 15 min. As increasing amounts of phospholipid were titrated into a FM1-43 solution, the fluorescence increased and finally reached a plateau value. Nearly all dye was bound to lipid vesicles.

UV measurements were performed with a Uvikon 860 (Kontron Instruments). The optical length of the cuvette was 1 cm. We determined the optical properties of FM1-43 in aqueous solution and bound to POPC vesicles. The absorption maximum, λ_{max}, and the extinction coefficient, ε_{max}, were 496 nm (476 nm) and 3.63×10^4 M^{-1} cm^{-1} (3.1×10^4 M^{-1} cm^{-1}), respectively for aqueous solutions (sonified POPC vesicles).

3. Results

3.1. Binding equilibrium studied with high sensitivity titration calorimetry and fluorescence spectroscopy

Using high sensitivity titration calorimetry we have measured the binding enthalpy of FM1-43 to sonified lipid vesicles as shown in Fig. 1A. The calorimeter cell contained sonified POPC vesicles ($c_L = 16$ mM) in buffer (100 mM NaCl, 10 mM Tris, pH 7.4) and 10-μl aliquots of a dye solution ($c_F = 1.13$ mM) in the same buffer were injected at 5-min intervals. The reaction was exothermic and the same heat of binding of $h_i = -24 \pm 1$ μcal was released in each injection. As a control, the same fluorophore solution was injected into buffer without lipid. The heat of dilution was small but was nevertheless included in the evaluation of the molar binding enthalpy ΔH. Assuming complete binding of the injected fluorophore to the lipid bilayer, the evaluation of Fig. 1A yields a binding enthalpy of $\Delta H = -2.3$ kcal/mol. The binding enthalpy was also measured at pH 5.5 and with mixed POPC/POPG vesicles. The data are summarized in Table 1. Only small variations in the binding enthalpy were observed with ΔH in the range of -2.3 kcal/mol $\leq \Delta H \leq -1.6$ kcal/mol. The dibutylaminostyryl group has a pK value of p$K \sim 5.1$ and is 30% protonated at pH 5.5 ($z = 2.3$). At pH 7.4 the dibutylaminostyryl group is deprotonated and the total charge is $z = +2$. The difference in charge has little influence on the binding enthalpy.

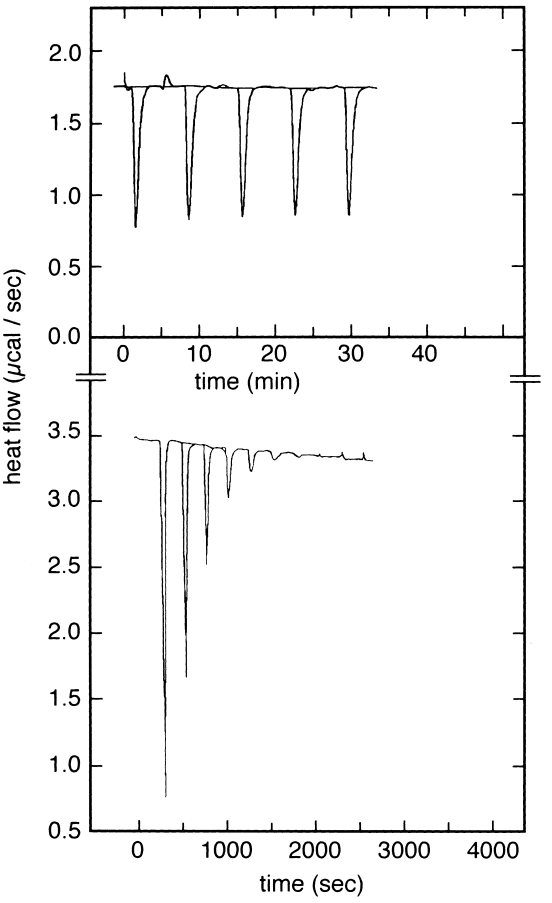

Fig. 1. Titration calorimetry of FM1-43 with lipid vesicles. Upper panel: Dye-into-lipid titration. The calorimeter cell (1.278 ml) contained sonified POPC vesicles ($c_L = 16$ mM) in buffer (10 mM Tris, 100 mM NaCl, pH 7.4). Each calorimeter tracing corresponds to the injection of 10 μl of an FM1-43 solution ($c_F = 1.13$ mM) in the same buffer. Lower panel: Lipid-into-dye titration. The calorimeter cell contained an FM1-43 solution (103 μM) which was titrated with sonified POPC/POPG (80/20 mol/mol) vesicles ($c_L = 42$ mM). Each titration peak corresponds to a 10-μl lipid injection. Both solutions were buffered as above. Measuring temperature 28°C.

Table 1
Reaction enthalpy, ΔH, for the binding of FM1-43 to sonified phospholipid vesicles (28°C, 10 mM Tris or phosphate, 100 mM NaCl)

Membrane composition (POPC/POPG in mol/mol)	Buffer	pH	ΔH (kcal/mol)
100/0[a]	Phosphate	5.5	−2.0
100/0[b]	Phosphate	7.4	−1.7
100/0[a]	Tris	7.4	−2.3
100/0[b]	Tris	7.4	−1.8
75/25[b]	Tris	7.4	−1.6
67/33[a]	Tris	7.4	−2.1

[a]Dye concentration determined by weight.
[b]Dye concentration determined by UV spectroscopy.

The binding isotherm was determined by a lipid-into-dye titration experiment as shown in Fig. 1B. The calorimeter cell contained the dye solution ($c_F = 103$ μM) in buffer (pH 7.4) and phospholipid vesicles were injected. Each calorimeter trace corresponds to the injection of 10 μl of sonified unilamellar POPC/POPG (80/20 mol/mol) vesicles at a lipid concentration of $c_L = 42$ mM. With each injection the amount of free dye available for lipid binding is reduced and the reaction enthalpy decreases gradually. The steepness of the decrease is a measure of the binding affinity (cf. Seelig, 1997).

Fig. 2A then shows the cumulative heat of reaction as a function of injection steps. The data can be used to derive the binding isotherm [22]. The binding isotherms determined for the binding of FM1-43 to pure POPC and mixed POPC/POPG vesicles are compared in Fig. 3. The degree of binding, X_b, is given as a function of the free dye concentration, c_{eq}, in equilibrium with the membrane phase. X_b is defined as the molar ratio of the amount of bound dye to the amount of lipid on the vesicle outside (60% of total lipid). It should be noted that FM1-43 cannot translocate into the inner monolayer because of its 2 positive charges. Obviously, the dye binds better to negatively charged POPC/POPG vesicles than to neutral POPC membranes. For both membranes the binding isotherm is non-linear.

Titration calorimetry was sensitive enough to measure binding isotherms down to total dye concen-

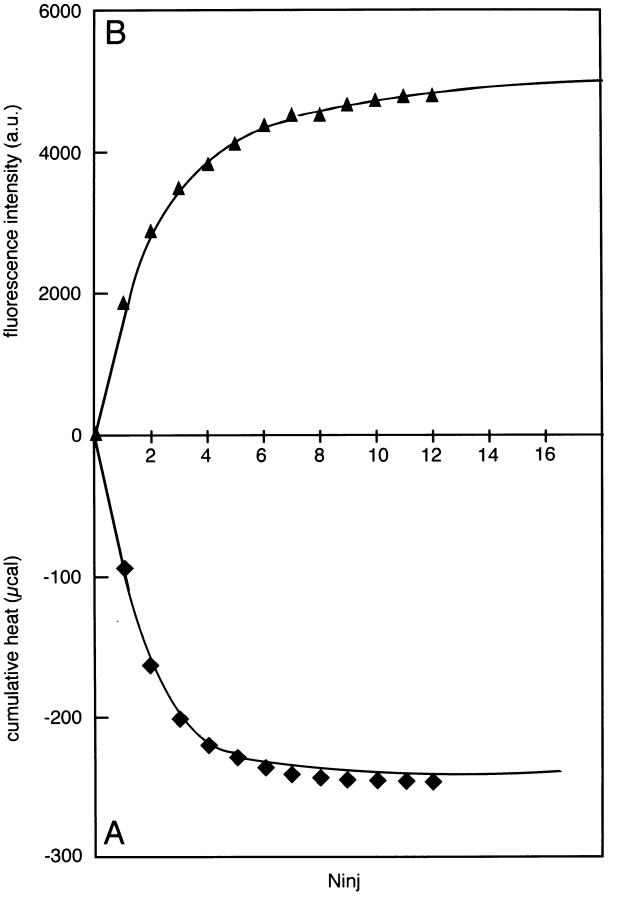

→

Fig. 2. Comparison of isothermal titration calorimetry (A) with fluorescence spectroscopy (B). In A the cumulative heat, $\Sigma_i h_i$, is shown as a function of the injection number N_{inj}. The experimental data, h_i, were taken from Fig. 1, lower panel. Panel B describes the variation of fluorescence intensity (arbitrary units) of FM1-43 upon addition of phospholipids. The quartz cuvette contained the dye solution at a concentration of $c_F = 1.8$ μM, i.e. the concentration is about a factor of 50 smaller than in A. The dye solution was titrated with sonified POPC/POPG vesicles (80/20 mol/mol) at a concentration $c_L = 3.5$ mM. Each data point corresponds to the consecutive injection of 10 μl lipid dispersion. The solid lines correspond to the theoretical titration curves calculated with $K = 6.35 \times 10^3$ M^{-1}, $z = 1.2$ and either $\Delta H = -1.86$ kcal/mol (A), or $F_\infty = 5000$ (B).

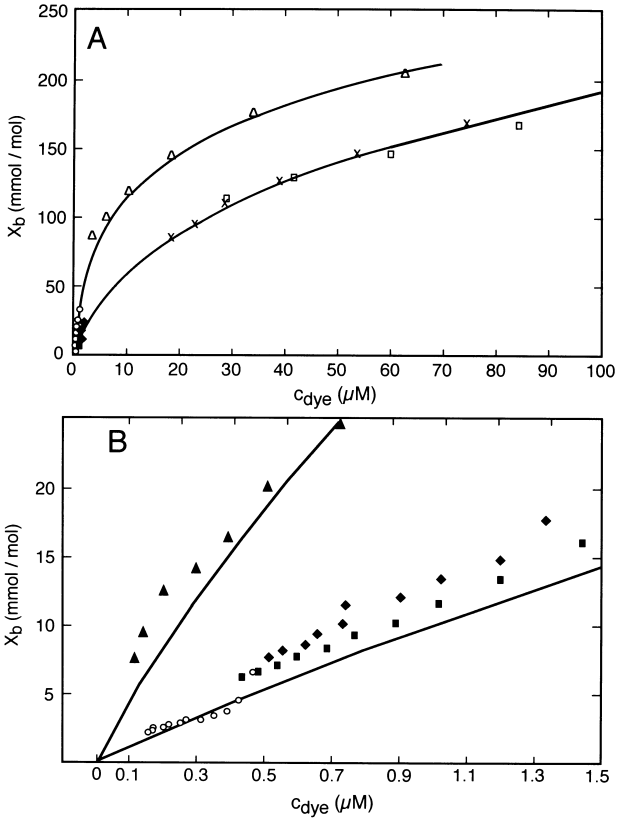

Fig. 3. Binding isotherms for the binding of FM1-43 to neutral and charged phospholipid bilayers. The degree of binding, X_b, defines the molar ratio of bound dye to total lipid in the outer monolayer. c_{Dye} is the equilibrium concentration of dye in bulk solution. A: High concentration range. Data with $c_{Dye} > 5$ μM were determined with titration calorimetry. B: Expanded view of the low concentration range. Data determined with fluorescence spectroscopy. The different symbols denote independent measurements at different concentrations. Binding to POPC vesicles is always weaker (lower X_b values) than binding to mixed POPC/POPG (80/20 mol/mol) vesicles. The solid line corresponds to theoretical binding isotherms calculated with $K = 1.15 \times 10^4$ M^{-1} and $z = 1.0$ for POPC vesicles (lower trace) and $K = 6.35 \times 10^3$ M^{-1}, $z = 1.2$, and $K_{Na} = 0.6$ M^{-1} for mixed POPC/POPG vesicles (upper trace).

tration $c_F^o > 100$ μM. The corresponding equilibrium concentrations were $c_{eq} > \sim 5$ μM. In Fig. 3A the data point at large dye concentrations ($c_{eq} > 5$ μM) and therefore refer to isothermal titration calorimetry. The low concentration data in the same figure were obtained with fluorescence spectroscopy. A 0.5–2-μM dye solution was filled in a quartz cuvette and was titrated with phospholipid vesicles. The emission maximum of FM1-43 in aqueous solution was at $\lambda_{max} = 629$ nm (10 mM Tris, 100 mM NaCl, pH 7.4, 25°C). The fluorescence properties of the dye were markedly altered upon addition of phospholipid vesicles. The emission maximum shifted to a shorter wavelength ($\lambda = 602$ nm) and the fluorescence intensity increased dramatically. Fig. 2B shows the variation of the fluorescence intensity at $\lambda = 602$ nm with the number of lipid injections. The fluorescence intensity reached a plateau value when all dye was bound to the lipid membrane. The fluorescence intensity thus paralleled the behavior of the cumulative heat (Fig. 2A). The fraction of bound dye, Θ_F, can be derived from the measured fluorescence intensity F_i (i = number of injections) according to

$$\Theta_F = \frac{F_i - F_0}{F_\infty - F_0} \quad (1)$$

where F_0 and F_∞ are the fluorescence intensities at the beginning and the end of the titration. F_i and F_∞ must be corrected for dilution effects. F_∞ can be estimated by a plot of $(F_i - F_0)^{-1}$ vs. $(c_L)^{-1}$ extrapolated to $(c_L)^{-1} \rightarrow 0$. Knowledge of Θ_F allows the evaluation of the free dye concentration in solution, c_{eq}, and, in turn, the calculation of the binding isotherm.

In the fluorescence experiments the dye was employed at concentrations about two orders of magnitude smaller than those used in titration calorimetry. This avoided self-quenching of the dye and was the concentration range usually employed in neurophysiological studies. The lipid concentration was also reduced by about one order of magnitude to achieve a reasonable resolution in the titration pattern.

The data points deduced from fluorescence measurements are included in Fig. 3A and constitute the low concentration range of the binding isotherm. Fig. 3B shows an expanded view of this part of the binding isotherm. The scatter of the data is considerable but an approximately linear relationship between bound dye and free dye in solution is observed for the initial part of the binding isotherms. The fluorescence data thus provide no insight into the exact binding mechanisms since most binding models degenerate into a linear binding isotherm at sufficiently low substrate concentrations.

3.2. Deuterium nuclear magnetic resonance

The influence of the dye on the structure of the

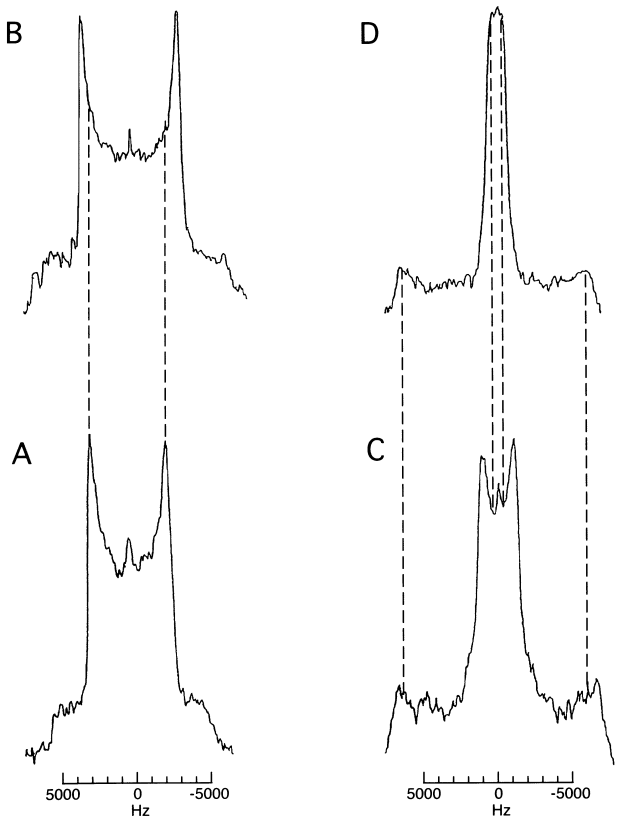

Fig. 4. Deuterium NMR spectra of POPC lipid membranes selectively deuterated at either the β-methylene (-NCD_2CH_2OP-) segment of the phosphocholine headgroup (A, B) or at the *cis*-double bond of the oleic acyl chain (C, D). The bottom spectra (A, C) correspond to pure POPC membranes in excess buffer. The top spectra were measured with FM1-43 present. The amount of bound dye was $X_b = 0.13$ (mol/mol) in spectrum C and $X_b = 0.16$ (mol/mol) in spectrum D. All measurements were made with coarse lipid dispersions.

lipid membrane was investigated with ^{2}H-NMR. The phosphocholine headgroup as well as the hydrophobic membrane interior were studied. To simplify the discussion the following nomenclature was introduced for the deuterated phosphocholine headgroup:

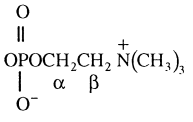

^{2}H-NMR spectra were obtained for the α- and β-headgroup segments and representative results are shown in Fig. 4A,B for the β-segment. The spectra are typical for liquid-crystalline bilayers [23]. They are characterized by a single quadrupole splitting indicating a single, time-averaged headgroup conformation at all dye concentrations. It is not possible to differentiate between free lipid and lipid bound to dye molecules. This result requires a rapid translational diffusion of the dye on the membrane surface, affecting all lipid headgroups to equal extent (with a residence time of less than 10^{-5} s at each headgroup).

A comparison of Fig. 4A and B demonstrates that the addition of FM1-43 increases the quadrupole splitting of the β-segment. In contrast, the quadrupole splitting of the neighboring α-segment decreases upon dye binding (spectra not shown). The variations of the quadrupole splittings $\Delta\nu_\alpha$ and $\Delta\nu_\beta$ of the two headgroup segments with the amount of surface bound dye, X_b, are summarized in Fig. 5. X_b is defined now as the molar ratio of bound dye to the total amount of lipid since the NMR probes were made by mixing dye and lipid in organic solution. Linear regression analysis of the spectral changes yields

$$\Delta\nu_\alpha = 6.1 - 17.2\ X_b\ (\text{kHz}) \quad (2)$$

$$\Delta\nu_\beta = 5.3 + 10.3\ X_b\ (\text{kHz}). \quad (3)$$

The variation of the quadrupole splitting is more pronounced at the α- than at the β-segment and the ratio of the slopes is $m_\beta/m_\alpha = -0.6$. The counter-di-

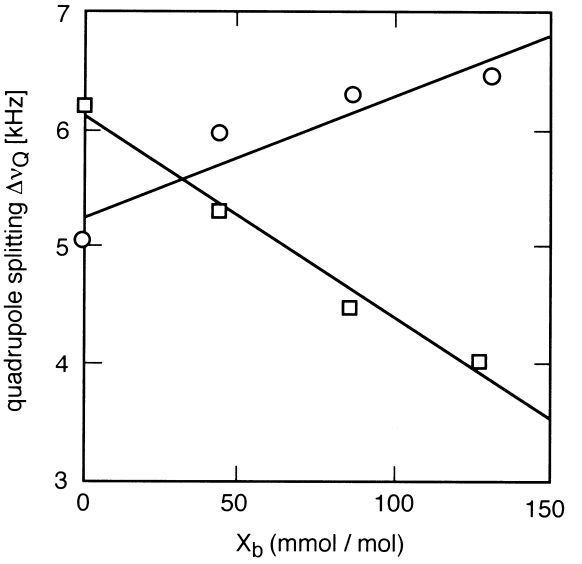

Fig. 5. Variation of the quadrupole splitting of pure POPC membranes selectively deuterated at the lipid head group segments (-NCD_2CD_2OP-), α-CD_2-POPC (□); (-NCD_2CH_2OP-), β-CD_2-POPC (○).

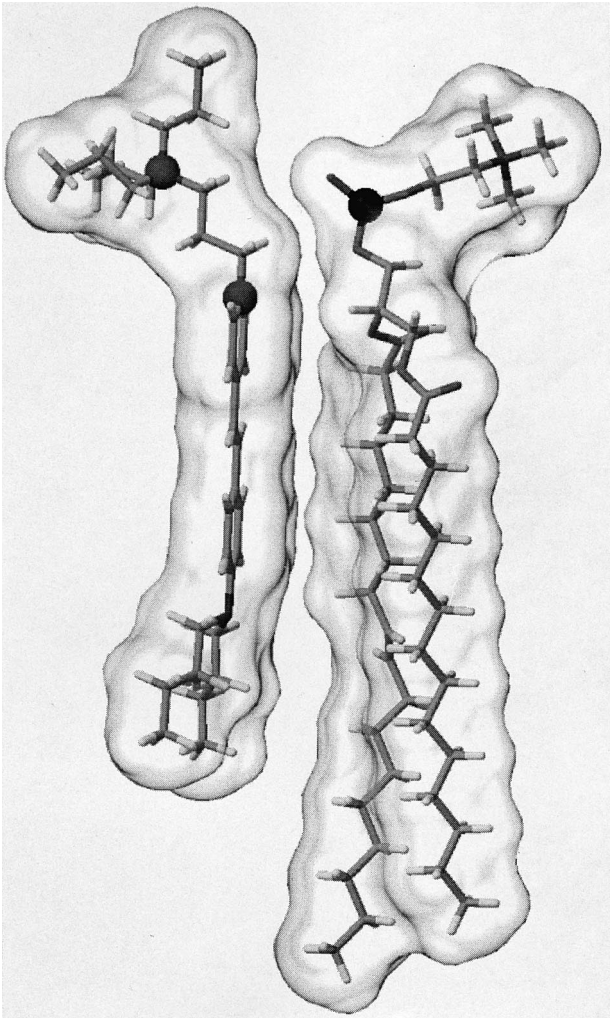

Fig. 6. Molecular models of FM1-43 (left) and POPC (right). The negative phosphate charge of POPC is positioned at approximately equal distance from the two quarternary ammonium charges of FM1-43.

rectional change of the two headgroup splittings can only be explained by a conformational change of the choline headgroup [24].

The influence of FM1-43 on the POPC hydrocarbon region was studied with selectively deuterated [9,′10′-$^2H_2$]POPC. The two deuterons are attached to the *cis*-double bond of the oleic acyl chain. In pure POPC membranes two different quadrupole splittings can be distinguished with separations of 13.1 kHz for the C-9 deuteron and 2.1 kHz for the C-10 deuteron (Fig. 4C) [19]. Addition of FM1-43 decreases both splittings (Fig. 4D). Again a linear variation of the quadrupole splittings with the amount of bound dye is observed with

$$\Delta\nu_9 = 13.1 - 4.6\ X_b \quad (4)$$

$$\Delta\nu_{10} = 2.1 - 8.8\ X_b. \quad (5)$$

The simultaneous decrease of both quadrupole splittings indicates a more disordered hydrocarbon chain conformation in the presence of dye. The relative change is larger for the C-10 deuteron than for C-9 deuteron even though the two deuterons are attached at the same *cis*-double bond. This phenomenon can be traced back to a tilting of the *cis*-double bond [19].

4. Discussion

4.1. Binding isotherms and thermodynamic parameters

The binding isotherms as deduced from titration calorimetry and fluorescence spectroscopy are summarized in Fig. 3. They were calculated with the assumption that FM1-43 binds to the outer lipid monolayer only (60% of total lipid). Since FM1-43 carries a net charge of $z = +2$ at physiological pH, a passive diffusion of the dye into the inner monolayer can be excluded. Inspection of Fig. 3 reveals that FM1-43 shows a higher affinity for negatively charged POPC/POPG vesicles than for neutral POPC vesicles which can be explained by electrostatic attraction. The initial parts of the binding isotherms are approximately linear (Fig. 3B) and can be used to derive an apparent binding constant, K_{app}, corresponding to a partition equilibrium of the form

$$X_b = K_{app} \cdot c_{eq} \quad (6)$$

with $K_{app} \sim 1.1 \times 10^4$ M^{-1} for POPC and $K_{app} \approx 4 \times 10^4$ M^{-1} for POPC/POPG (80/20) vesicles.

A physically more realistic interpretation of the binding isotherm must differentiate between electrostatic attraction/repulsion and chemical adsorption. Due to electric charge effects the concentration of the cationic dye near the membrane surface is different from that in bulk solution. For a negatively charged membrane the dye concentration at the membrane surface, c_M, is considerably higher than

the equilibrium concentration in bulk solution, c_{eq}, and can be calculated according to

$$c_M = c_{eq} e^{-zF_0\psi_0/RT} \quad (7)$$

where z is the valency of the dye, F_0 is the Faraday constant, and ψ_0 the membrane surface potential at the plane of binding. For a membrane surface potential of $\psi_0 = -50$ mV the surface concentration of the dye is larger by a factor of ~ 50 (~ 7) for $z = +2$ ($z = +1$) compared to the bulk concentration.

Electrostatic effects also play a role for non-charged POPC vesicles. Insertion of the cationic dye into the neutral membrane imparts a positive charge onto the outer monolayer. Dye molecules in solution will be repelled and the membrane surface concentration is smaller than the bulk concentration. Again the Boltzmann (Eq. 7) is valid. However, at very low dye concentrations the difference between c_M and c_{eq} becomes negligible and the binding constant can indeed be derived from the tangent to the binding isotherm at the origin. For the POPC binding isotherm shown in Fig. 3 this leads to $K_0 = 1.15 \times 10^4$ M^{-1} as mentioned above. K_0 is a true measure of the chemical affinity of the dye towards the membrane. At higher dye concentrations the apparent binding constant will decrease continuously.

A different situation is encountered for negatively charged POPC/POPG vesicles. At low dye concentrations the membrane surface charge exerts its maximum effect. The initial K_{app} of 4×10^4 M^{-1} thus comprises electrostatic and chemical (hydrophobic) free energy contributions. Increasing the free dye concentration gradually reduces the electric charge of the membrane surface due to dye binding. At electric neutrality, electric charge contributions can be neglected and the free dye concentration corresponds to K_0^{-1} (if Na^+ binding is neglected). However, the binding isotherm as such provides no obvious indication where electroneutrality is reached. Instead a detailed analysis of the binding isotherm using the Gouy-Chapman theory is required.

The details of this approach have been described previously in connection with peptide-membrane interactions [17] and the present analysis proceeds in an analogous manner. The electric surface charge of the membrane vesicles is determined as the difference between the negative charge of the lipid and the positive charge of bound dye and bound Na^+. Dye binding is essentially hydrophobic and involves the whole lipid matrix; Na^+ binding is limited to the PG headgroup and is described with a Langmuir adsorption isotherm assuming a PG/Na^+ stoichiometry of 1:1 and an Na^+ binding constant of $K_{Na^+} = 0.6$ M^{-1}. The Gouy-Chapman theory provides a relationship between the surface charge density, the membrane surface potential, and the ion distribution. The binding isotherms calculated with this approach are given by the solid lines in Fig. 3.

Let us first analyze the binding of FM1-43 to neutral bilayers. As discussed above, the intrinsic binding constant can be derived from the low concentration regime without invoking the Gouy-Chapman theory. The experimental data shown in Fig. 3 are best represented by $K_0 = 1.15 \times 10^4$ M^{-1}. The remaining free parameter in the Gouy-Chapman approach is the electric charge of the binding molecule. For FM1-43 under physiological conditions a charge of $z = 2$ is expected since the tertiary amino group has a pK of 5.1 and is not protonated. A simulation of the high concentration range of the binding isotherm with $z = 2$ is, however, unsatisfactory. The calculated X_b values are distinctly too small. An optimum fit of the experimental data requires a smaller effective charge and the theoretical binding curve shown in Fig. 3 was, in fact, calculated with $z = 1$. Analogous discrepancies between the true charge of a molecule and its effective charge in the Gouy-Chapman approach have been noted before, mainly for proteins. This is usually explained by the spatial distribution of the relevant charges such that a simultaneous contact of all charges of a given protein with the membrane surface is not possible. However, the two positive charges in FM1-43 are separated in the linear molecule by at most ~ 5 Å which is less than the Debye length of 9.3 Å under the present conditions. Both charges should therefore be sensed by the membrane surface. However, a partial screening of these charges can be induced by a rather specific alignment of the dye with respect to the phosphocholine dipole layer. This alignment is suggested by the ^{2}H-NMR data (see below) and is illustrated in Fig. 6. The non-charged part of the dye molecule is shown to penetrate into the hydrophobic part of the lipid bilayer, in agreement with the experimental evidence obtained with fluorescence spectroscopy. More important, the two positive charges of the dye are postu-

lated to have a rather specific location: in Fig. 6 they are placed at approximately equal distance above and below the plane of the phosphate groups. The pyridinium charge is below the phosphate anion, closer to the bilayer center. It is thus screened from the aqueous phase by a layer of phosphate groups leaving only the second quaternary ammonium group accessible at the membrane outside. The electrostatic repulsion induced by the cationic dye would thus be caused only by the more distal charge, in agreement with $z \sim 1$ as deduced from the Gouy-Chapman theory.

We may now proceed to negatively charged membrane surface of POPC/POPG vesicles. The intrinsic binding cannot be determined directly from the binding isotherm but requires the use of the Gouy-Chapman theory. The best fit to the experimental data as shown in Fig. 3 was found for $K_0 = 6.45 \times 10^3$ M^{-1} and $z = 1.2$. The error in both parameters is estimated to be 20%. In spite of the distinctly higher affinity of FM1-43 to POPC/POPG vesicles the chemical (hydrophobic) binding constant is smaller compared to that of pure POPC vesicles. The larger X_b values can therefore be traced back exclusively to electrostatic attraction.

The free energy of hydrophobic binding is hence rather similar for the two membrane systems. It can be calculated according to $\Delta G = -RT \ln(55.5\ K_0)$ where the factor 55.5 accounts for the cratic contribution [25]. For FM1-43, ΔG falls in the range of -8.0 kcal/mol (POPC) to -7.7 kcal/mol (POPC/POPG). Since the binding enthalpy is $\Delta H \approx -2$ kcal/mol the dominant contribution to ΔG is the entropy term with $T\Delta S \sim 6.0$ kcal/mol. Hence the association of FM1-43 with the lipid membrane is an entropy-driven reaction.

The dye FM2-10 is more hydrophilic than FM1-43 since its non-polar hydrocarbon chains contain only two instead of 4 methylene/methyl units. FM2-10 was shown to have a much faster destaining rate than FM1-43 [11]. We have measured the binding of FM2-10 to POPC/POPG (80/20 mol/mol) vesicles and measured a binding enthalpy of $\Delta H = -2.3$ kcal/mol which is similar to that of FM1-43. However, the apparent binding constant was distinctly lower with $K_{app} \sim 1000$–3000 M^{-1} at 1 μM and K_0 also reduced to $K_0 \sim 200$ M^{-1}. The lower affinity to the membrane explains the faster dissociation rate of FM2-10 since the association rate of FM1-43 and FM2-10 should be identical.

4.2. Dye location in the lipid membrane

Upon binding to POPC vesicles the dye molecule experiences a dramatic shift in its spectral properties. The fluorescence intensity increases about 50–100-fold and the fluorescence emission maximum shows a blue-shift of 27 nm. In the ground state most of the positive charge is concentrated in the pyridinium ring; it is shifted to the aminophenyl end upon excitation [26]. Since the excited state is stabilized only by polar solvents the blue shift provides evidence for the location of the chromophore in a non-polar environment. Fluorescence polarization spectroscopy further suggests that the chromophore is oriented perpendicular to the membrane surface, i.e. with its long axis parallel to the fatty acyl chains [26]. In the present study the same shift in wavelength is seen for POPC and mixed POPC/POPG vesicles. Apparently the electrostatic interaction with the negatively charged POPC/POPG does not change the location of the chromophore in the membrane.

The insertion of the dye molecule into the hydrophobic region is reflected in the ^{2}H-NMR spectra of POPC deuterated at the *cis*-double bond. FM1-43 is a semi-rigid, linear molecule with two bulky ring systems which does not fit smoothly between the parallel fatty acyl chains. The perturbation of the lipid packing increases the segmental fluctuations and decreases the quadrupole splittings. This is in contrast, for example, to the insertion of cholesterol which produces an increase in the quadrupole splittings of the *cis*-double bond by up to 100% due to the stiffening of the hydrocarbon chains in the presence of the flat and rigid steroid frame [27,28]. However, an increase in statistical disorder alone is not sufficient to explain the spectral changes observed in Fig. 4. The molecular origin of the two separate splittings of the *cis*-double bond is a tilting of the C=C axis with respect to the bilayer normal by about 7–8° [19]. If the C=C axis is exactly parallel to the bilayer normal the two deuterons would give rise to exactly the same splitting. The two quadrupole splittings can thus be changed not only by an increase or decrease in the statistical disorder but also by a change in the tilt angle. Statistical disorder

will affect both splittings to equal extent, a change in the tilt angle, however, will favor one deuteron over the other. Comparison of Eqs. 4 and 5 demonstrates that the C-10 quadrupole splitting varies faster than the C-9 splitting, indicating an increase in tilt angle superimposed on a decrease in bilayer ordering. Fig. 6 shows that FM1-43 is too short to span the monolayer. In order to fill the vacant space in the central bilayer region the fatty acyl chains must twist around the aromatic aminophenyl ring changing, in turn, the average orientation of the *cis*-double bond.

More specific information on the location of FM1-43 with respect to the plane of the membrane comes from the ^{2}H-NMR data of the phosphocholine headgroup. Neutron diffraction [29] and ^{2}H- and ^{31}P-NMR studies [30] have demonstrated that the $^-$P-N$^+$ dipoles of phosphatidylcholine membranes are extended essentially parallel to the membrane surface. This is further supported by a theoretical analysis of headgroup interactions in monolayer and bilayer systems [31,32]. In this model even a small 'backward' orientation is predicted with the N$^+$ end moving towards the hydrocarbon phase.

Addition of FM1-43 to the POPC membrane has opposite effects on the two choline segments: the α-splitting decreases and the β-splitting increases. This finding is in qualitative agreement with many other positively charged compounds which bind to the membrane surface [33] and can be explained by a rotation of the $^-$P-N$^+$ dipole away from the membrane with the N$^+$ end moving closer to the water phase [24]. The variation of the quadrupole splittings with the amount of bound dye is summarized by Fig. 5 and Eqs. 2 and 3. The slopes m_i thus provide a quantitative measure of the efficacy of the membrane-bound molecule to change the quadrupole splitting and, in turn, the orientation of the phosphocholine headgroup. The monovalent local anesthetic dibucaine, for example, has a slope of $m_\alpha = -28.8$ kHz/mol and $m_\beta = +14$ kHz/mol [34], melittin with an effective charge of $z = 2.2$ yields $m_\alpha = -93.3$ kHz/mol and $m_\beta = 44.4$ kHz/mol [35]. The modest efficacy of FM1-43, in spite of its charge $z = +2$, in changing the headgroup conformation ($m_\alpha = -17.2$ kcal/mol; $m_\beta = 10.3$) is thus surprising. A simple explanation is provided, however, by placing the two charges of FM1-43 as indicated in Fig. 6. In this configuration the negative phosphocholine phosphate group is sandwiched between the two positive quaternary amino charges, one above, the other below the plane of the $^-$P-N$^+$ dipoles. The two charges counteract each other, at least partially, and thus inhibit a large rotation of the $^-$P-N$^+$ dipole. On the other hand, the charge compensation is not perfect since a limited rotation of the $^-$P-N$^+$ dipole towards the water phase does occur as evidenced by the ^{2}H-NMR spectra.

4.3. Concluding remarks

FM1-43 penetrates easily into neutral and anionic lipid membranes with about the same hydrophobic binding constant. The binding affinity is modulated by electrostatic attraction/repulsion and FM1-43 at low dye concentration binds distinctly better to anionic membranes. The depth of penetration into the hydrophobic part is determined by the location of the two quaternary ammonium groups of FM1-43. For POPC membranes the two cationic charges are above and below the plane containing the $^-$P-N$^+$ dipoles. The position of these charges could change in other membranes, varying the penetration depth of FM1-43. This could explain, in part, the different spectral properties of FM1-43 in different cell types.

Acknowledgements

We thank H. Reuter for bringing this problem to our attention and for constructive criticism. We are indebted to R. Dutzler for the computer graphics of Fig. 6. Supported by the Swiss National Science Foundation Grant 31.42058.94.

References

[1] A.S. Waggoner, Annu. Rev. Biophys. Bioeng. 8 (1979) 47–68.
[2] L.M. Loew, G.W. Bonneville, J. Surow, Biochemistry 17 (1978) 4065–4071.
[3] L.M. Loew, L.L. Simpson, Biophys. J. 34 (1981) 353–365.
[4] A.S. Waggoner, A. Grinvald, Ann. NY Acad. Sci 303 (1977) 217–241.
[5] A. Grinvald, R. Hildesheim, I.C. Farber, L. Anglister, Biophys. J. 39 (1982) 301–308.

[6] W.J. Betz, F. Mao, C.B. Smith, Curr. Opin. Neurobiol. 6 (1996) 365–371.
[7] W.J. Betz, G.S. Bewick, Science 255 (1992) 200–203.
[8] W.J. Betz, G.S. Bewick, J. Physiol. (London) 460 (1993) 287–309.
[9] W.J. Betz, F. Mao, G.S. Bewick, J. Neurosci. 12 (1992) 363–375.
[10] T.A. Ryan, H. Reuter, B. Wendland, F.E. Schweizer, R.W. Tsien, S.J. Smith, Neuron 11 (1993) 713–724.
[11] T.A. Ryan, S.J. Smith, H. Reuter, Proc. Natl. Acad. Sci. USA 93 (1996) 5567–5571.
[12] T.A. Ryan, H. Reuter, S.J. Smith, Nature 388 (1997) 478–482.
[13] D. Sulzer, E. Holtzman, J. Neurocytol. 18 (1989) 529–540.
[14] L.M. Loew, L.B. Cohen, B.M. Salzberg, A.L. Obaid, F. Bezanilla, Biophys. J. 47 (1985) 71–77.
[15] A. Grinvald, R.D. Frostig, E. Lieke, R. Hildesheim, Physiol. Rev. 68 (1988) 1285–1366.
[16] S. McLaughlin, Annu. Rev. Biophys. Biophys. Chem. 18 (1989) 113–136.
[17] J. Seelig, S. Nebel, P. Ganz, C. Bruns, Biochemistry 32 (1993) 9714–9721.
[18] L.K. Tamm, J. Seelig, Biochemistry 22 (1983) 1474–1483.
[19] J. Seelig, N. Waespe-Sarcevic, Biochemistry 17 (1978) 3310–3315.
[20] J.H. Davis, K.R. Jeffrey, M. Bloom, M.J. Valic, T. Higgs, Chem. Phys. Lett. 42 (1976) 390–394.
[21] T. Wiseman, S. Williston, J.F. Brandts, L.N. Lin, Anal. Biochem. 179 (1989) 131–137.
[22] J. Seelig, Biochim. Biophys. Acta 1331 (1997) 103–116.
[23] J. Seelig, Q. Rev. Biophys. 10 (1977) 353–418.
[24] J. Seelig, P.M. Macdonald, P.G. Scherer, Biochemistry 26 (1987) 7535–7541.
[25] C.R. Cantor, P.R. Schimmel, Biophysical Chemistry, Vol. 1, Freeman, San Francisco, CA, 1980.
[26] L.M. Loew, L. Simspon, A. Hassner, V. Alexanian, J. Am. Chem. Soc. 101 (1979) 5439–5440.
[27] B. Bechinger, J. Seelig, Chem. Phys. Lipids 58 (1991) 1–5.
[28] R.G. Habiger, J.M. Cassal, H.J. Kempen, J. Seelig, Biochim. Biophys. Acta 1103 (1992) 69–76.
[29] G. Büldt, H.U. Gally, J. Seelig, G. Zaccai, J. Mol. Biol. 134 (1979) 673–691.
[30] J. Seelig, G.U. Gally, R. Wohlgemuth, Biochim. Biophys. Acta 467 (1977) 109–119.
[31] D. Stigter, K.A. Dill, Langmuir 4 (1988) 200–209.
[32] K.A. Dill, D. Stigter, Biochemistry 27 (1988) 3446–3453.
[33] G. Beschiaschvili, J. Seelig, Biochim. Biophys. Acta 1061 (1991) 78–84.
[34] A. Seelig, P.R. Allegrini, J. Seelig, Biochim. Biophys. Acta 939 (1988) 267–276.
[35] E. Kuchinka, J. Seelig, Biochemistry 28 (1989) 4216–4221.